

# A boundary element and level set based bi-directional evolutionary structural optimisation with a volume constraint

BaseerUllah<sup>a,\*</sup>, JonTrevelyan<sup>b</sup>, Siraj-ul-Islam<sup>a</sup>

<sup>a</sup>*University of Engineering and Technology, Peshawar, Pakistan.*

<sup>b</sup>*School of Engineering and Computing Sciences, Durham University,  
South Road, Durham DH1 3LE, UK.*

---

## Abstract

A new topology optimisation algorithm is implemented and presented for compliance minimisation of continuum structures using a volume preserving mechanism which effectively handles a volume constraint. The volume preserving mechanism is based on a unique combination of the level set method and a boundary element based bi-directional evolutionary structural optimisation approach using a bisectioning algorithm. The evolving structural geometry is implicitly represented with the level sets, efficiently handling complex topological shape changes, including holes merging with each other and with the boundary. Numerical results for two-dimensional linear elasticity problems suggest that the proposed adaptation provides smooth convergence of the objective function and a more robust, smoother geometrical description of the optimal design. Moreover, this new implementation allows for efficient material re-distribution within the design domain such that the

---

\*Corresponding author

*Email address:* [baseerullah@gmail.com](mailto:baseerullah@gmail.com) (BaseerUllah)

objective function is minimised at constant volume. The proposed volume preserving mechanism can be easily extended to three-dimensional space.

*Keywords:* topology optimisation, boundary element method, level set method, BESO

---

## 1. Introduction

The main goal of structural optimisation is to provide an optimal design which should effectively comply to its intended objectives and at the same time satisfies the constraints imposed upon it. The demand for low-cost, light weight and high performance structures can be addressed through the development of high performance structural optimisation methods. Among the three types of structural optimisation, i.e. size, shape and topology, topology optimisation is the most beneficial from economic perspective and the most challenging from engineering perspective. According to [1], topology optimisation methods can be broadly classified into density based and level set based methods. In density based methods, the geometry of the structure is represented through a material distribution of two or more phases, e.g. [2, 3], etc. In the second category an implicit boundary description is used to represent the structural geometry, e.g. [4, 5, 6, 7, 8], which are based on the level set method (LSM) [9].

In the LS based optimisation techniques, the performance of an evolving structural geometry can be evaluated using different geometry mapping approaches. According to [1], the most commonly used approaches are immersed boundary and conforming discretisation. There also exists another approach, where a fixed Eulerian mesh can be used for the LSM implemen-

tation and a body conforming approach for the evolution of the structural response. The body conforming approach can be based either on:

- the finite element method (FEM) based domain discretisation
- the boundary element method (BEM) based boundary only discretisation

The reduction of problem dimensionality with the use of BEM based body conforming mapping is very attractive as compared to the FEM based domain discretisation. In the literature of structural optimisation, researchers combined the BEM with the LSM for the solution of optimisation problems in both two and three-dimensions, e.g, compliance minimisation [10, 11, 12, 13], sound scattering [14, 15], heat conduction [16], etc.

An improvement in the structural performance of a candidate design can be based either on the shape sensitivity information (e.g. [6, 17, 18, 19]) or through an evolutionary approach based on a criterion such as von Mises (e.g. [4, 20]). The basic concept of evolutionary structural optimisation (ESO) is based on the progressive removal of inefficient materials, which evolves the structure towards an optimum [21, 22]. The bi-directional evolutionary structural optimisation (BESO) presented in [23] also allows for efficient material to be added at the same time as the inefficient material is removed.

The removal and addition of materials in most of the finite element (FE) based BESO approaches are linked with the element removal and addition, which provides optimal designs with checkerboard patterns and jagged edges. Therefore, filtering process is always required to minimise the occurrence of these undesirable effects [24, 25]. In the boundary element (BE) based BESO

approaches [26, 27] the material removal is accomplished through hole insertion and boundary movements, and addition through boundary movements only. However, due to the explicit geometry representation adopted in [26], special care is always required when hole merges with each other and with the boundary. The BE based BESO approach has been further integrated with the LSM for the solution of both two and three-dimensional optimisation problems in [12, 28], which allows for the complex topological changes to take place automatically. As reported in the literature, the BE based BESO approaches largely eliminate the common problems occur in the FE based approaches, e.g. checkerboard patterns, jagged edges and mesh dependency. However, these methods are based on the target volume based stopping criterion instead of the most desirable, i.e. the minimisation of the objective function at constant volume criterion, which would provide optimal designs with improved performance.

A new optimisation method presented in this paper is based on a compliance minimisation objective function with a volume constraint, for linear elastic problems. In order to exactly satisfy the volume constraint, a novel methodology has been proposed for the constant volume preserving mechanism within the BEM and LSM framework. The proposed implementation exactly satisfies the volume constraint and, in addition, allows us to monitor the structural performance through a direct measurement of the compliance at constant volume during the optimisation process. The volume preserving mechanism is based on the bisectioning algorithm, which precisely adjusts the material removal in accordance with the material addition.

The effectiveness of the proposed implementation is thoroughly evaluated

through the numerical examples presented and it has been observed that this new algorithm provides smooth convergence of the objective function and better geometrical description of the final design, i.e., the optimal geometries produced are smoother, and have more uniformly sized members, than those reported in [20, 21, 26, 28]. In addition, this new implementation allows us to evaluate its intended purpose of minimising the objective function at constant volume, which is of a paramount importance for designing high performance structures. Therefore, this is a clear advantage of this method over the those presented in [20, 26, 28], where the optimal designs are based on the minimisation of the specific strain energy without incorporating the constant volume constraint. Hence, in each of the optimisation problem considered in this study, the performance of the proposed implementation is exceptional and the minimisation of compliance at constant volume has also been accomplished.

This paper is organised as follows. In section 2, we discuss the BE and LS based BESO approach. In Section 2.5 the implementation details of the volume preserving algorithm are presented. The optimisation procedure is provided in Section 3. In Section 4, we present numerical examples, and discuss the performance of the proposed optimisation method. The paper closes with some concluding remarks in Section 5.

## **2. The BE and LS based BESO approach**

A classical problem in structural optimisation is to find the stiffest structure with a given volume of the material. According to the BESO approach, a structure can be optimised through the progressive removal of inefficient

and addition of efficient materials based on the sensitivity information. In the current implementation the design sensitivities are evaluated through the BEM and the LSM is then used to evolve the structural geometry in accordance with the BESO criterion. The integration of the various numerical techniques used in this study is discussed in detail as follows.

### 2.1. Problem statement

In the current implementation the design objective is to find the optimal topology of a structure with minimum compliance subject to a volume constraint. Consider an elastic structure with analysis domain  $\Omega$  and boundary  $\Gamma$ . The boundary  $\Gamma$  is decomposed such that

$$\Gamma = \Gamma_0 \cup \Gamma_1 \cup \Gamma_2 \quad (1)$$

where  $\Gamma_0$  corresponds to regions having Dirichlet boundary conditions (where displacements are zeros),  $\Gamma_1$  corresponds to non-homogeneous Neumann boundary conditions (where tractions are prescribed) and  $\Gamma_2$  corresponds to homogeneous Neumann boundary conditions (traction free).  $\Gamma_0$  and  $\Gamma_1$  are fixed and  $\Gamma_2$  is allowed to vary during the optimisation process.

The optimisation problem can be expressed as finding  $\Gamma_2$  to minimise the compliance (i.e. a measure of the strain energy), subject to the volume constraint. Mathematically, the optimisation problem can be stated as:

$$\begin{aligned} \text{Minimise: } J(u) &= \int_{\Gamma} \frac{1}{2} t_i u_i d\Gamma & (2) \\ \text{Subject to: } G &= \int_{\Omega} d\Omega - V_t = 0 \end{aligned}$$

where  $t_i$  and  $u_i$  are the traction and displacement in the direction  $i$ , and  $V_t$  is the target volume.

According to the BESO concept, the low sensitivity (stress or strain energy) regions within a structure reflect the inefficient material utilisation and the high sensitivity regions indicate insufficient material. Therefore, the progressive removal and addition of material in the BESO based optimisation method allows efficient material re-distribution for the prescribed volume of the material, accompanied with minimisation of the objective function. Hence, this provides optimum structure with near the same (safe) sensitivity (stress, strain energy) level.

### *2.2. Boundary element analysis*

The BEM is used as a structural analysis tool in the current implementation. Due to the boundary only discretisation the structural response can be directly evaluated at the nodal points associated with the elements. Moreover, in a BE analysis stresses (or any other required property) inside the design domain can be calculated at internal points as a post processing step. The current implementation uses the boundary element analysis software Concept Analyst (CA) [30]. Therefore, the complete optimisation code is fully integrated within the CA.

### *2.3. Design sensitivity analysis*

In most of the FE based BESO approaches the removal and addition of materials is linked with the element removal and addition, which provides optimal designs with checkerboard patterns and jagged edges. Therefore, additional measures are always adopted to minimise the occurrence of these undesirable effects. However, in the BE based BESO approaches [26, 28] the material removal is accomplished through hole insertion and boundary

movements, and addition through boundary movements only, without any undesirable effects. The topological and shape sensitivities have been used to identify regions within the structure to be modified accordingly.

In the current implementation, both these sensitivities are based on the von Mises stress criterion, which drive the removal and addition process in order to achieve a minimum of the objective function. According to the comparative study presented in [30], the criterion of von Mises stress in the classical ESO method is equivalent (empirically) to the compliance minimisation criterion, and that the compliance minimisation problem can be solved by directly using the von Mises stress criterion, and vice versa.

### *2.3.1. Topological sensitivity*

The material removal inside the design domain is based on the hole nucleation around internal points with the lowest value of the von Mises stress ( $\sigma_V$ ). This indicates that the structural material has not been efficiently utilised at the low stressed regions and can be removed accordingly. As proposed in [20], hole nucleation takes place around internal points which satisfy the following condition,

$$\sigma_{Vi} \leq f_V \sigma_{Vmin} \quad (3)$$

where  $\sigma_{Vi}$  is the von Mises stress at a given internal point,  $\sigma_{Vmin}$  is the minimum value of von Mises stress over all internal points in the current iteration, and  $f_V$  is the von Mises stress threshold factor. The hole insertion mechanism and selection of  $f_V$  are discussed in details in [20].

### 2.3.2. Shape sensitivity

The von Mises stress has also been used as a criterion for shape sensitivity information, i.e. to identify regions of low stress, where material will be removed, and regions of high stress, where material will be added. The removal and addition of material can be carried out through inward and outward boundary movements, respectively, as proposed in [28]. Therefore, boundary nodes with low and high stress values are identified as follows,

- $\sigma_{V_n} < 0.9 RR \sigma_{V_r}$  : remove material
- $\sigma_{V_n} > \min(\sigma_{V_r}, \sigma_Y)$  : add material

where  $\sigma_{V_n}$  is the von Mises stress at a given boundary node,  $RR$  is the removal ratio,  $\sigma_Y$  is the material's Yield stress, and  $\sigma_{V_r}$  is the reference von Mises stress. In the current implementation,  $\sigma_{V_r} = \sigma_{V_{max}}$ , where  $\sigma_{V_{max}}$  is the maximum von Mises stress in the initial design. Once the low and high stressed nodes are identified the LSM is then used to evolve the structural geometry.

### 2.4. Representation and evolution of the structural geometry

In the current implementation, the shape and topology of the evolving structural geometry are represented through an implicit function  $\phi$ , defined as the signed distance of a particular point grid point from the boundary. Mathematically,  $\phi$  can be expressed as follows:

$$\phi(\vec{x}) \begin{cases} < 0 & \vec{x} \in \Omega \text{ (inside)} \\ = 0 & \vec{x} \in \partial\Omega \text{ or } \Gamma \text{ (boundary)} \\ > 0 & \vec{x} \notin \Omega \text{ (outside)} \end{cases} \quad (4)$$

The level set function  $\phi$  can be evolved through the solution of a Hamilton-Jacobi (HJ) equation [9]

$$\frac{\partial \phi}{\partial t} + F|\nabla \phi| = 0 \quad (5)$$

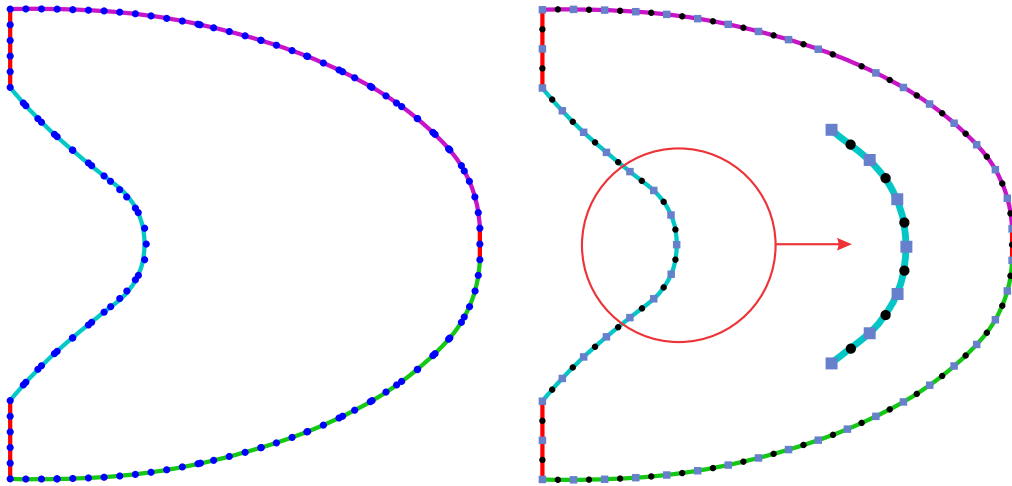
where  $F$  is the velocity in the normal direction and  $t$  is the virtual time.

The structural optimisation problem can be solved by providing appropriate velocity values of  $F$  for use in Equation (5). Therefore,  $F$  is computed from the structural response at the boundary. Based on the discussion in Section 2.3.2, the von Mises stress at each node point is converted into a scaled velocity through a stress velocity relationship presented in [28] as given below:

- $\sigma_{Vn} \in [0, \sigma_{t1}] : \sigma_{t1} = 0.5 RR \sigma_{Vr}, F = -1$
- $\sigma_{Vn} \in [\sigma_{t1}, \sigma_{t2}] : \sigma_{t2} = 0.9 RR \sigma_{Vr}, F \in [-1, 0]$
- $\sigma_{Vn} \in [\sigma_{t2}, \sigma_{t3}] : \sigma_{t3} = 0.95 \min(\sigma_{Vr}, \sigma_Y), F = 0$
- $\sigma_{Vn} \in [\sigma_{t3}, \sigma_{t4}] : \sigma_{t4} = \min(\sigma_{Vr}, \sigma_Y), F \in [0, 1]$
- $\sigma_{Vn} \in [\sigma_{t4}, \infty) : F = 1$

Once the boundary velocity is calculated for each node point, the same is extended to the level set grid using the method of Adalsteinsson and Sethian [32]. In the next step, the level set function is updated through the solution of Equation (5) with an upwind finite difference approximation [33]. The value of the time step size used is based on the Courant-Friedrichs-Lewy (CFL) condition.

During the optimisation process, at each iteration, the solution of Equation (5) updates  $\phi(\vec{x})$ , which allows us to modify the structural geometry. The  $\phi(\vec{x}) = 0$  contours (which represent the boundary of the modified geometry) are traced in accordance with the contour tracing algorithm presented in [28]. Further, non-uniform rational B-splines (NURBS) [34] are fitted through the zero level set intersection points which belong to  $\Gamma_2$  (i.e. the modifiable line segments in Figure 1(a)) as proposed in [28]. The automatic meshing facility



(a) NURBS through the zero level set intersection points

(b) NURBS discretised with boundary elements

Figure 1: Example of a reconstructed geometry for a cantilever beam

within CA is used to define elements on each spline, i.e. Figure 1(b), using a setting which is designed to produce peak stresses to approximately 1% accuracy, either with uniformly distributed boundary elements or with grading as required for good BEM meshing practice.

It should be noted that with a NURBS based geometry representation, the BE meshing can be carried out independently of the level set grid size. Thus the algorithm separates the BE mesh density from the LS grid size used to determine the underlying geometry and allows accurate stress solutions even using a coarse LS grid. Hence, this provides the freedom to use a suitable grid size based on the required accuracy and computational efficiency during the numerical implementation of the proposed method. Additionally, the structural geometry is always represented in a standard CAD format.

### *2.5. Implementation of the constant volume constraint*

In this new implementation, a three step approach is proposed to add and remove material at constant volume. Based on the von Mises stress distribution within the design domain at a given iteration, the algorithm calculates the amount of material which can be removed in the first step. The amount of material which can be added is calculated in the second step. In the third step, a bisectioning algorithm is used to adjust the removal and addition at the same rate. Hence, this provides an efficient mechanism which effectively preserves the required volume thereby exactly satisfying the volume constraint.

The first step of this algorithm is implemented as follows:

1. Set  $\bar{\phi} = \phi$ .
2. After the BE analysis, select all those nodes along the structural boundary with

$$\sigma_V \leq \sigma_{t2} \tag{6}$$

where  $\sigma_{t2}$  is the stress level as defined in Section 2.4; assign velocity  $F = -1$  to all those nodes.

3. Extend velocities as assigned in step 2 to grid points in the narrow band and update  $\bar{\phi}$ , i.e.

$$\frac{\partial \bar{\phi}}{\partial t} + F|\nabla \bar{\phi}| = 0 \quad (7)$$

4. Calculate the new volume  $V_1$ . The material removed around the low stressed nodes, i.e.  $V_R$  is given as

$$V_R = V - V_1 \quad (8)$$

where  $V$  is the volume calculated before the level set update.

The amount of material which can be added is calculated in the second step as follows:

1. Set  $\bar{\phi} = \phi$ .
2. Using the same BE analysis results as in (6) select all those nodes with

$$\sigma_V \geq \sigma_{t3} \quad (9)$$

where  $\sigma_{t3}$  is the stress level as defined in Section 2.4; assign velocity  $F = 1$  to all those points.

3. Extend velocities as assigned in the previous step and solve Equation (7).
4. Calculate the new volume  $V_2$ . The material added around the high stressed nodes, i.e.  $V_A$  is given as

$$V_A = V_2 - V \quad (10)$$

In some cases if the material addition is very low, i.e.  $V_A < 1.0$ , then the expression of  $\sigma_{t3}$  is relaxed through a factor  $R_A$  as follows

$$\sigma_{t3} = (0.95 - R_A) \min(\sigma_{Vmax}, \sigma_Y) \quad (11)$$

where  $R_A = 0.1$ , and is incremented by 0.1 until sufficient material addition takes place, i.e. as per Equation (10)  $V_A \geq 1.0$ .

During the numerical implementation, it has been observed that  $V_R$  is always greater than  $V_A$ . Two options may be considered to make the material addition and removal at the same rate:

- Increase  $V_A$  while  $V_R$  is fixed
- Decrease  $V_R$  while  $V_A$  is fixed

However, it can be seen that the material addition takes place with  $F = 1$ , and if the material addition rate is increased in accordance with the removal rate, then it requires that  $F > 1$ , and in some cases this may violate the CFL condition. However, if the removal rate is decreased in accordance with the addition rate, then  $F < 1$ , and in this case the CFL condition will always be satisfied. Therefore, in the third step a bisectioning algorithm is used to adjust the material removal in accordance with the material addition such that a constant volume is maintained. Two additional factors are introduced, i.e.  $l_{Rm1}$  and  $l_{Rm2}$  which bounds  $l_{Rm}$ . The complete algorithm is explained in the following steps.

1. Initialise  $l_{Rm1} = 0$  and  $l_{Rm2} = 1$
2. Set  $\bar{\phi} = \phi$

3. Halve the interval, i.e.

$$l_{Rm} = (l_{Rm1} + l_{Rm2})/2 \quad (12)$$

4. Assign velocity  $F = -l_{Rm}$  to all those points according to Equation (6).
5. Extend velocities to grid points in the narrow band.
6. Solve Equation (7) and calculate the new volume  $V_3$ .
7. Calculate  $V_R = V - V_3$
8. if  $V_A \leq V_R$ ,  $l_{Rm2} = l_{Rm}$  else  $l_{Rm1} = l_{Rm}$ .
9. Terminate if  $|V_A - V_R| \leq 10^{-2}$ , otherwise go to step 2.

The implementation of the above algorithm provides an efficient mechanism which exactly satisfies the volume constraint in the proposed BE and LSM based BESO method.

The three-dimensional BEM and LSM based BESO approach for a specific strain energy objective function without a constant volume implementation has been studied in the authors previous work as reported in [12]. Where it has been shown that the proposed approach can be easily extended to three-dimensions. Firstly due to the natural extension of the LSM from two to three-dimensional space [33]. Secondly, the LSM efficiently handles shape and topology optimisation simultaneously through automatic hole nucleation by the intersection of two approaching surfaces [35]. Hence, the constant volume preserving mechanism can be easily extended to three-dimensional structural optimisation problems.

### 3. Optimisation algorithm

The proposed optimisation algorithm is illustrated in Figure 2 and summarised as follows:

1. Define structural geometry with applied loads and constraints.
2. Initialize level set grid with signed distance function to represent structural geometry implicitly.
3. Trace the zero level set contours and convert them into a standard CAD representation, i.e. NURBS.
4. Carry out boundary element analysis (BEA).
5. Check for hole nucleation; in case of hole nucleation go to step 4, otherwise go to step 6.
6. Compute velocity at each node point of the structural boundary using the BE analysis results.
7. Extend boundary velocities to level set grid points in the narrow band.
8. Solve Equation (5) to update the level set function.
9. Repeat the above procedure from step 3, until the stopping criterion is satisfied.

### 4. Examples and discussion

The validity and efficiency of the proposed optimisation method with a constant volume preserving algorithm are tested against some benchmarking problems in the field of structural optimisation. The material properties and various evolutionary factors used in these examples are:

- Poisson's ratio = 0.3

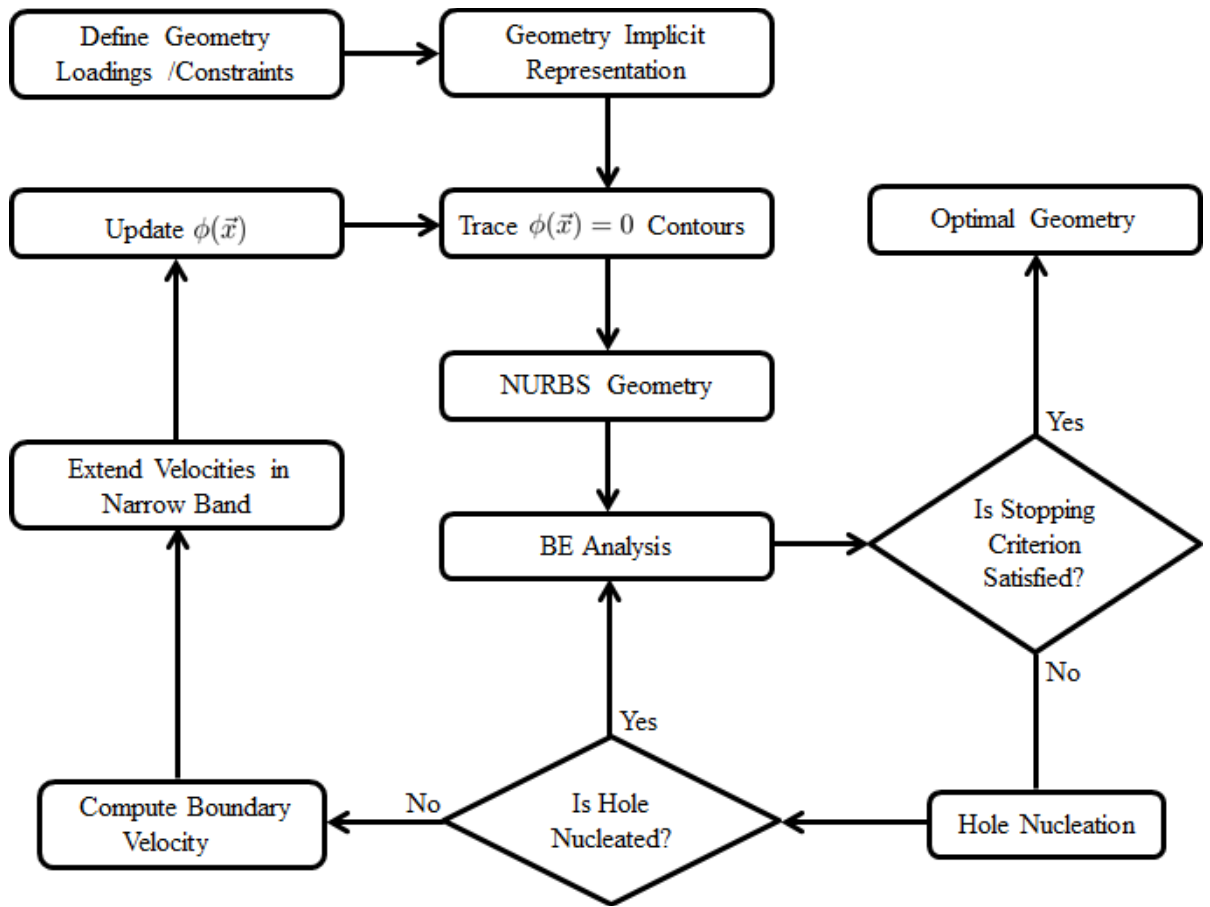


Figure 2: Optimisation flow chart

- Young's modulus = 210 GPa
- Yield stress = 280 MPa
- $RR = 0.01$

Plane stress conditions are assumed with arbitrary thickness of 1 mm. All examples are solved with a load  $P = 100$  N. In order to allow for a little growth in the problem geometry as the optimisation progresses, a fixed level

set domain is used during the numerical implementation with size slightly larger than the initial design domain. The optimisation process terminates when the relative difference between the compliances of the five successive iterations is less than  $10^{-2}$  or when the given maximum number of iterations has been reached.

#### 4.1. Example-1

The first example considered in this study is a cantilever beam of aspect ratio 1:1. The initial design with applied load and boundary conditions is shown in Figure 3(a). The structure is constrained at the top and bottom of the left hand edge with zero displacement boundary conditions and the load  $P$  is applied at the right hand side of the bottom edge. The optimisation problem is solved for a target volume  $V = 0.35V_0$  using three different choices of the initial guessed design;  $V_0$  is the volume of the initial design domain. The level set design domain is discretised with  $40 \times 40$  square cells.

Figure 3 shows the evolution history of the short cantilever beam starting from a completely filled initial design. During the optimisation process hole nucleation can be observed at different iterations. The value of hole nucleation factor used in this case is  $f_{VM} = 1.2$ .

The evolution of the compliance and volume fraction for the short cantilever beam at different stages of the optimisation process is depicted in Figure 4. The optimisation process starts from a completely filled initial design domain, hence the volume of the initial design domain is considerably greater than the target volume. In order to reach the target volume fraction the proposed optimisation method allows material removal from the low stressed regions of the structure through boundary movements and hole nucleation.

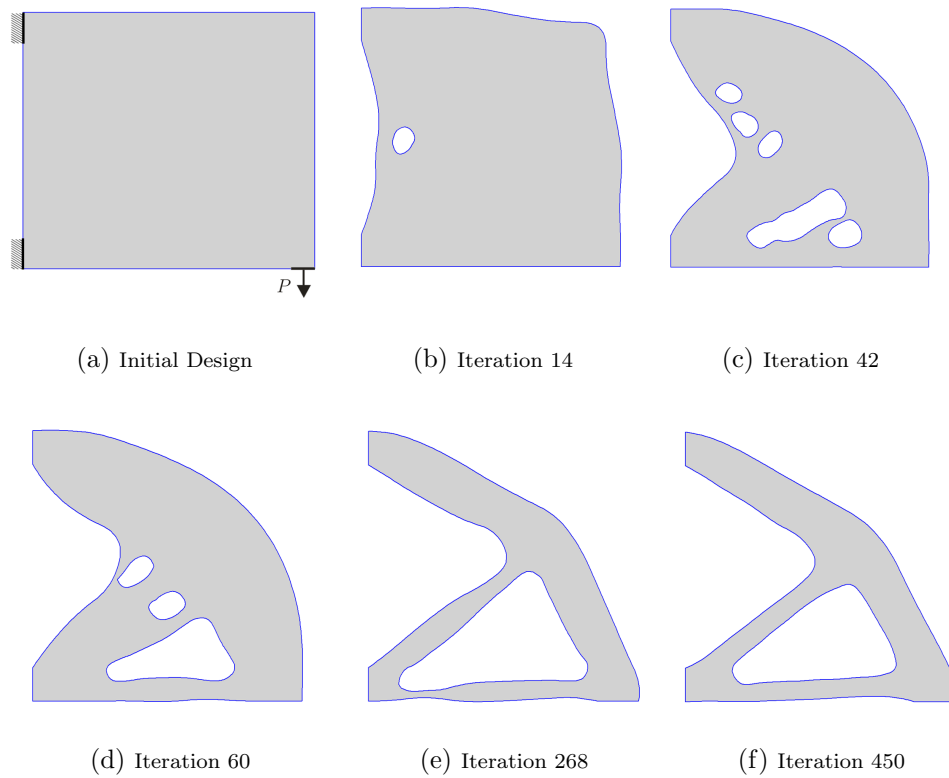


Figure 3: Evolution of structural geometry for Example-1, initial design without pre-existing holes

As a result the compliance increases initially up to iteration 268, where the structure volume reaches the target volume, and the volume constraint is exactly satisfied. Afterwards, the proposed volume preserving mechanism allows the optimisation process to be carried out at constant volume. It can be seen that once the volume constraint is satisfied the compliance initially decreases and then remains stable up to the end of the optimisation process. The optimisation process terminates when there is no further improvement in the compliance of the structure.

As discussed above the implementation of a constant volume preserv-

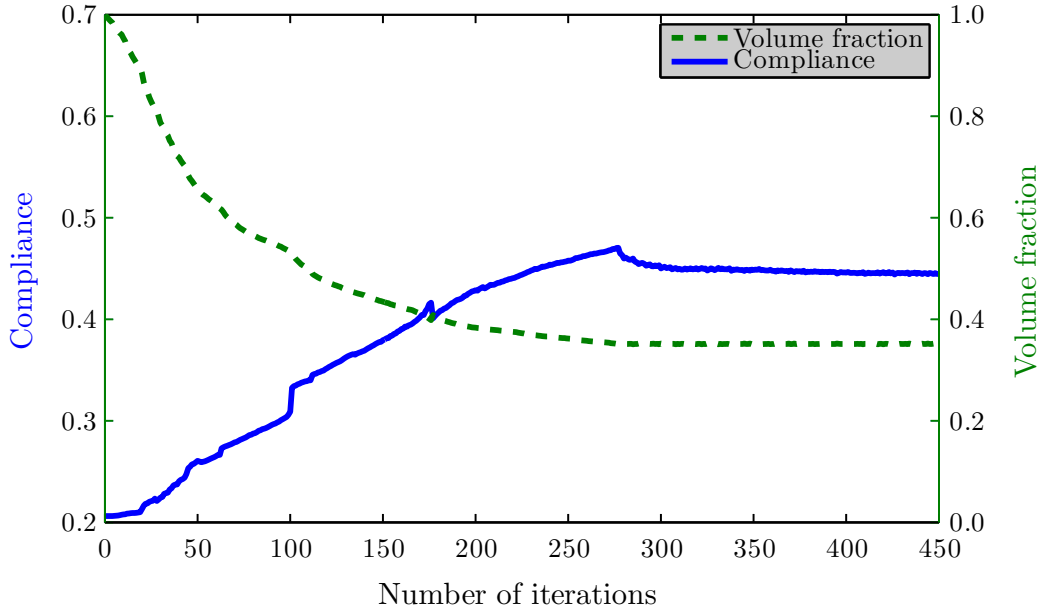


Figure 4: Convergence of objective function and volume for Example-1

ing mechanism exactly satisfies the volume constraint during the optimisation process. Further, the effectiveness of this new implementation can be evaluated by comparing Figures 3e (the structure volume reaches the target volume with compliance around 0.48), and 3f (the optimisation process terminates with compliance 0.442). It is evident from the optimal structural geometry at iteration 450 that the non-uniformity in sizes of the structural members at iteration 268 is effectively reduced through material redistribution at constant volume. This suggests that the proposed volume preserving mechanism redistributes material within the design domain such that the compliance is minimised at constant volume, and a more realistic optimal geometry is obtained. Hence, in the absence of a volume preserving mechanism, a sub-optimal design with non-smooth geometry would evolve.

In order to further validate the proposed optimisation method, four different tests are carried out for the optimisation of the short cantilever beam considering different initial designs and hole nucleation options; Table 1 shows a comparison of these results.

In case-1, the optimisation process starts from a completely filled initial design and here there is no hole nucleation. The volume convergence takes place at iteration 2700 and compliance convergence occurs at iteration 3500, respectively.

In case-2, the addition of hole nucleation greatly accelerates the optimisation process and the compliance convergence takes place at iteration 450. A comparison of the final compliance values of case-1 and 2 suggests that the use of hole nucleation mechanism not only provides fast convergence of both the compliance and volume fraction, but also provides optimal designs with improved performance.

In order to evaluate the sensitivity of the proposed method to the selection of initial guessed designs, in case-2, 3 and 4, different initial designs are considered, respectively. The result displayed in Table 1 suggests, that the final optimal designs and compliance are very close to each other. Further, the final optima are very similar to those available in the literature for this type of benchmark example (e.g. [36]). This suggests that the proposed optimisation method is insensitive to the selection of different initial designs.

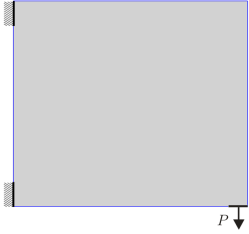
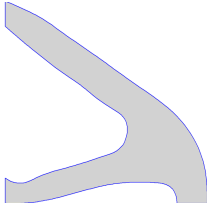
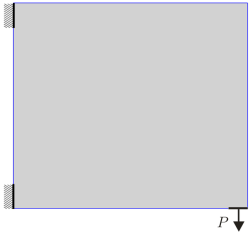
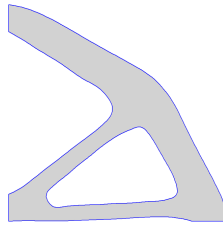
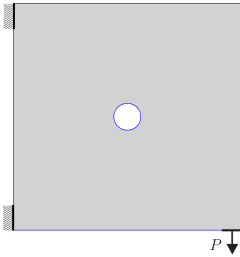
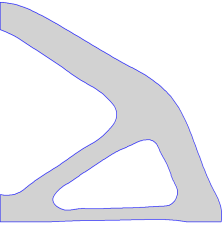
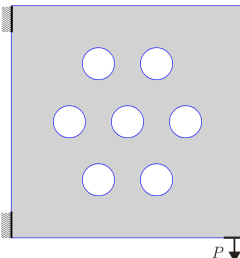
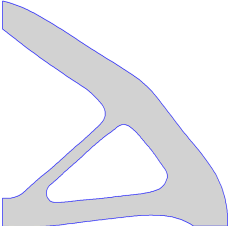
Case No	Initial Design	Final Design	HN	$NI_V$	$NI_C$	Complian
1			NO	2700	3500	0.465
2			YES	280	450	0.442
3			YES	107	300	0.442
4			YES	125	300	0.442

Table 1: Results comparison with different initial designs and hole nucleation options for Example-1; HN: Hole Nucleation option (YES/NO),  $NI_V$ : Number of iterations at volume convergence,  $NI_C$ : Number of iterations at compliance convergence

#### 4.2. Example-2

In the second example, the minimum compliance problem is solved for a cantilever beam of aspect ratio 1.5:1. Zero displacement boundary conditions are prescribed at the top and bottom portions of the left hand edge and the structure is loaded at the centre of the right edge as shown in Figure 5(a). The specified target volume fraction for this example is  $V = 0.35V_0$ . The level set design domain is discretised with  $60 \times 40$  square cells.

In this example an initial design completely filled with material is considered, and hole nucleation is allowed using  $f_{VM} = 1.6$ . The evolution of the structural geometry at various stages of the optimisation process is depicted in Figure 5. Nucleation of holes can be observed in Figure 5(b-e). The optimisation process comprised of hole insertion, evolution of both external and internal boundaries, and merging of holes with each other and with the boundary. Hence, both shape and topological changes take place simultaneously during the solution of the minimum compliance problem. The final optimum is very similar to that presented in [10, 11]

The evolution of the objective function and volume fraction at each iteration is depicted in Figure 6. Since the initial design domain is completely filled with material, the optimisation process starts from a minimum value of the objective function. Then it slowly increases as a result of the material removal through boundary movements and hole insertion. A jump in the compliance can be observed at iteration 16, which is mainly related to the removal of material through insertion of a hole slightly larger than normal. The two peaks recorded around iteration 107 and 120, respectively, can be related to the removal of structural members through hole merging as shown

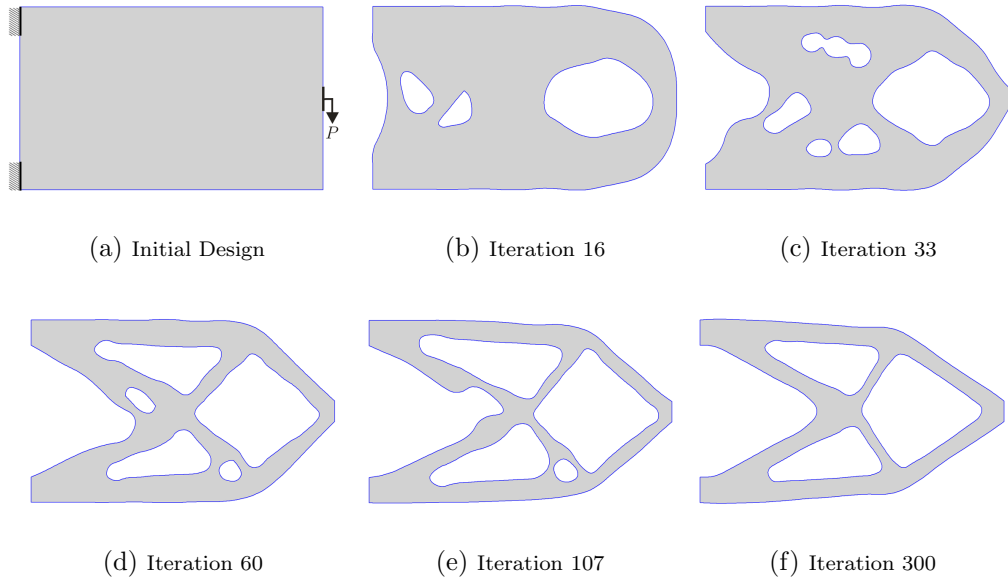


Figure 5: Evolution of structural geometry for Example-2

in Figure 5(e). In the subsequent iterations the effect of these peaks dies out quickly. Once the volume constraint is exactly satisfied, the objective function is gradually reduced and the optimisation process terminates at iteration 300, when the stopping criterion is satisfied.

It can be seen from Figure 6, that the structural volume reaches the target volume around iteration 107 (Figure 5e) with a maximum value of the structural compliance. However, the implementation of the volume preserving mechanism then lowers the compliance through material redistribution within the structural geometry. Further, this new implementation also allows topological changes to take place at constant volume through hole merging (in this case at iteration 120), with a slight increase in structural compliance. In the subsequent iterations the structural performance is further improved with a better description of the optimal geometry, i.e uniformity in the size of

each structural member. This uniformity in structural members sizes would not be achieved without using the constant volume preserving mechanism. This suggests that the implementation of the volume preserving mechanism is absolutely essential for high performance structural description.

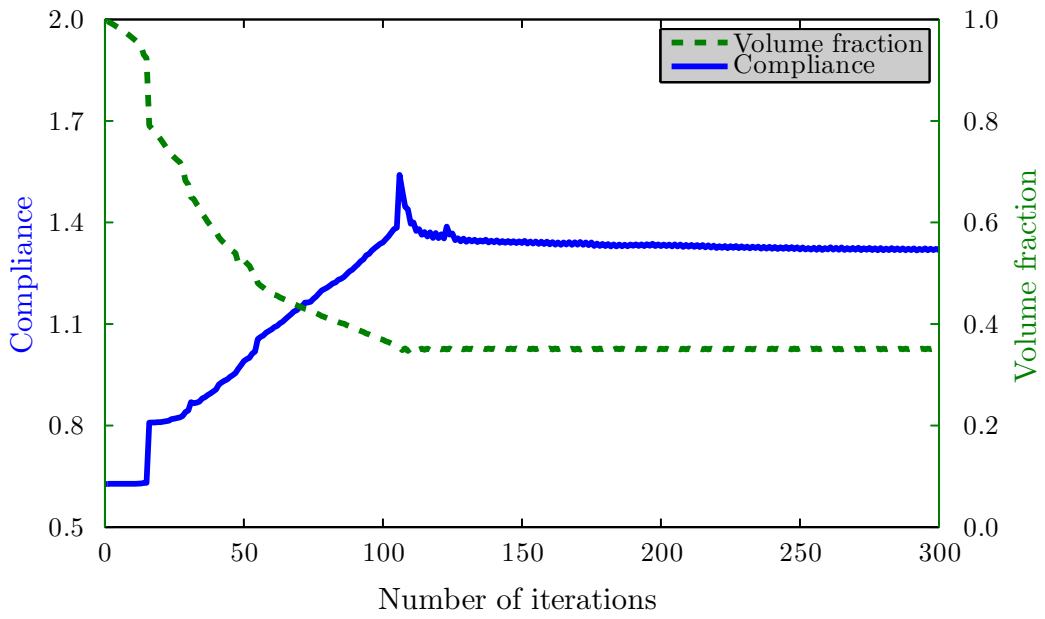


Figure 6: Convergence of objective function and volume for Example-2

### 4.3. Example-3

This example considers a cantilever beam of aspect ratio 3:1. The specified target volume fraction for this example is  $V = 0.4V_0$ . The level set design domain is discretised with  $90 \times 30$  square cells. The minimum compliance problem is solved for an initial design as shown in Figure 7(a); zero displacements boundary conditions are applied at the top and bottom portions of the left hand edge and the load  $P$  is applied at the right hand side of the bottom edge. The hole insertion factor used in this example is  $f_{VM} = 1.2$ . Nucleation of holes and their evolution afterwards allow hole merging with each other and with the boundary as depicted in Figure 7. This demonstrates that the current optimisation method has the capability to carry out both shape and topology optimisation simultaneously. The optimal design closely resembles that presented for a similar problem in [24].

The evolution histories of the objective function and the structural volume fraction at each optimisation iteration are depicted in Figure 8. The optimisation process starts from a minimum value of the objective function, a slow increase in the initial iterations is followed by a rapid increase after iteration 45. This increase in the compliance is mainly due to the material removal through insertion of large number of holes as can be seen in Figure 7(c). The volume constraint is satisfied around iteration 140. In the subsequent iterations, the volume preserving mechanism redistributes material within the design domain and reduces the structural compliance. The high peak at iteration 162 is due to the removal of a structural member through hole merging (see Figure 7(g)). The effect of this peak dies out quickly. The structural performance is further improved through the final iterations, and

the variation in some of the structural members size is minimised. A comparison of the structural geometry description at iteration 162 and 300 (Figure 7) clearly demonstrates the effectiveness of the volume preserving mechanism implemented in this study.

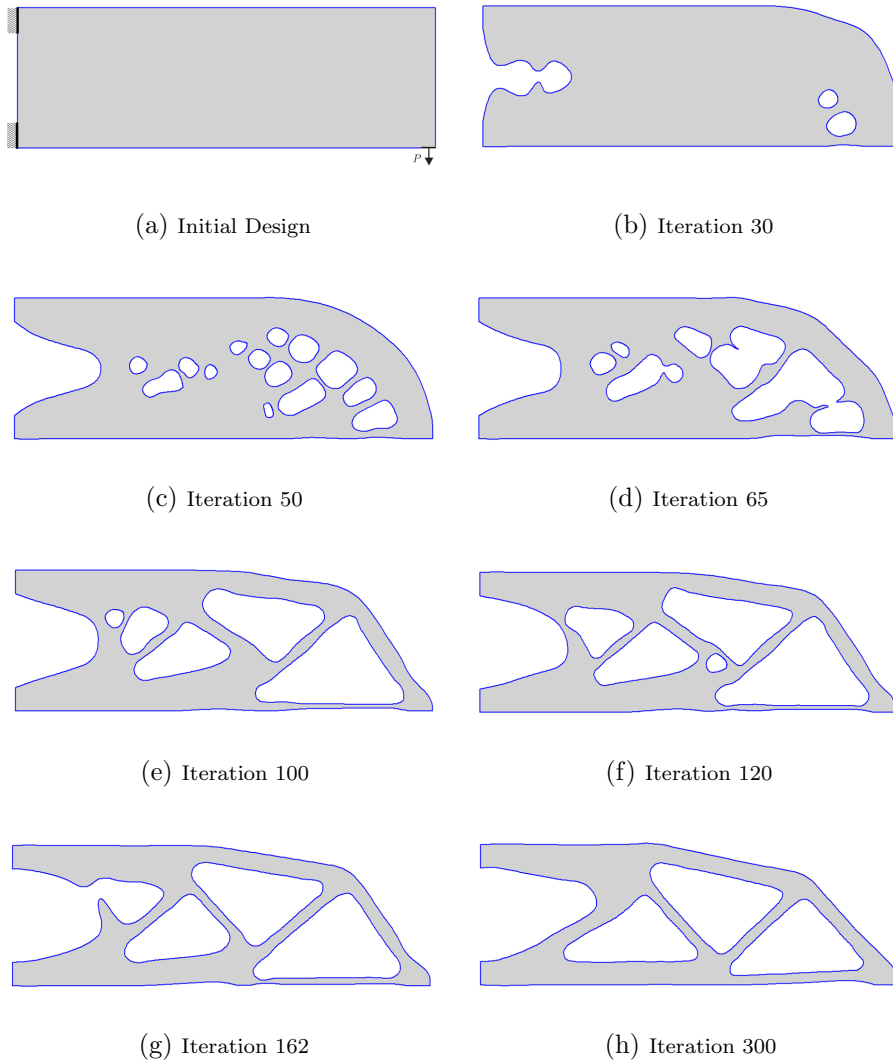


Figure 7: Evolution of structural geometry for Example-3

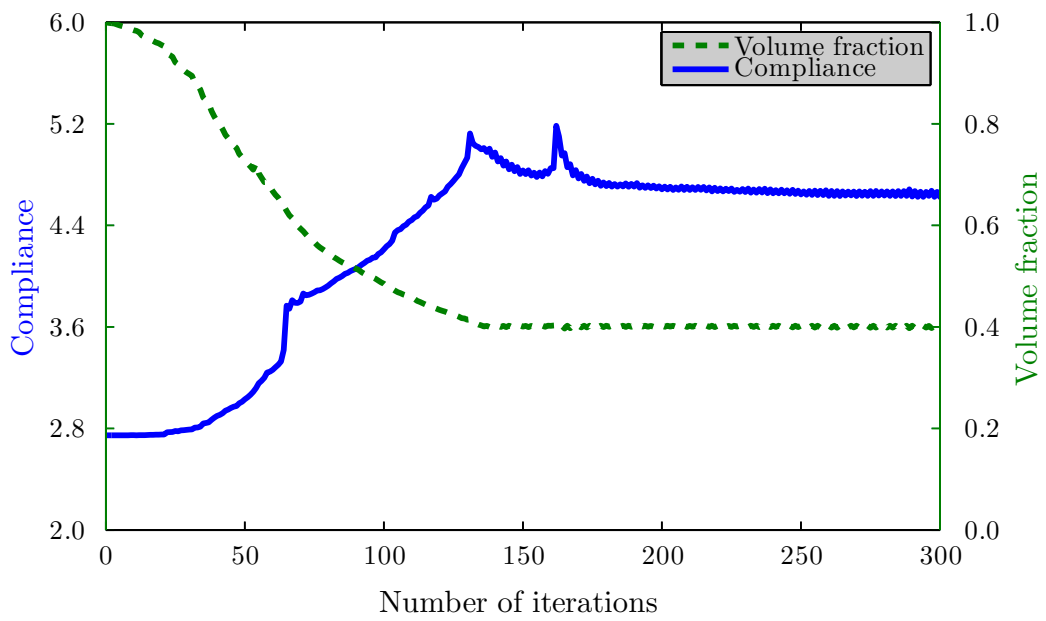


Figure 8: Convergence of objective function and volume for Example-3

#### 4.4. Example-4

The final example considered in this study is the Michell's type structure as shown in Figure 9(a) of aspect ratio 2:1. Zero displacement boundary conditions are applied in all directions at some portions of the left and right hand sides of the bottom edge, and a downward load  $P$  is applied at midspan along the bottom edge. The level set design domain is discretised with  $80 \times 40$  square cells. The minimum compliance problem is solved for a target volume of  $V = 0.35V_0$ . The evolution of the structural geometry, which is mainly comprised of hole insertion and evolution of both internal and external boundary, at different stages of the optimisation process is depicted in Figure 9. The evolution of the objective function and structural volume fraction for the Michell's type structure are depicted in Figure 10. In the initial iterations, the material removal through hole nucleation and boundary movements raises the compliance and at iteration 180 the compliance reaches its maximum value. Afterwards, the implementation of the volume preserving mechanism progressively enhances the structural performance through the minimisation of compliance at constant volume. This enhancement can also be validated from the comparison of Figure 10e and f, where the optimal design has a smoother and more uniformly sized structural members. Again, it can be seen that the use of such an optimisation algorithm without the constant volume adaptation can result in suboptimal designs. Hence, a constant volume preserving mechanism should be an essential part of structural optimisation algorithm for obtaining high performance structures.

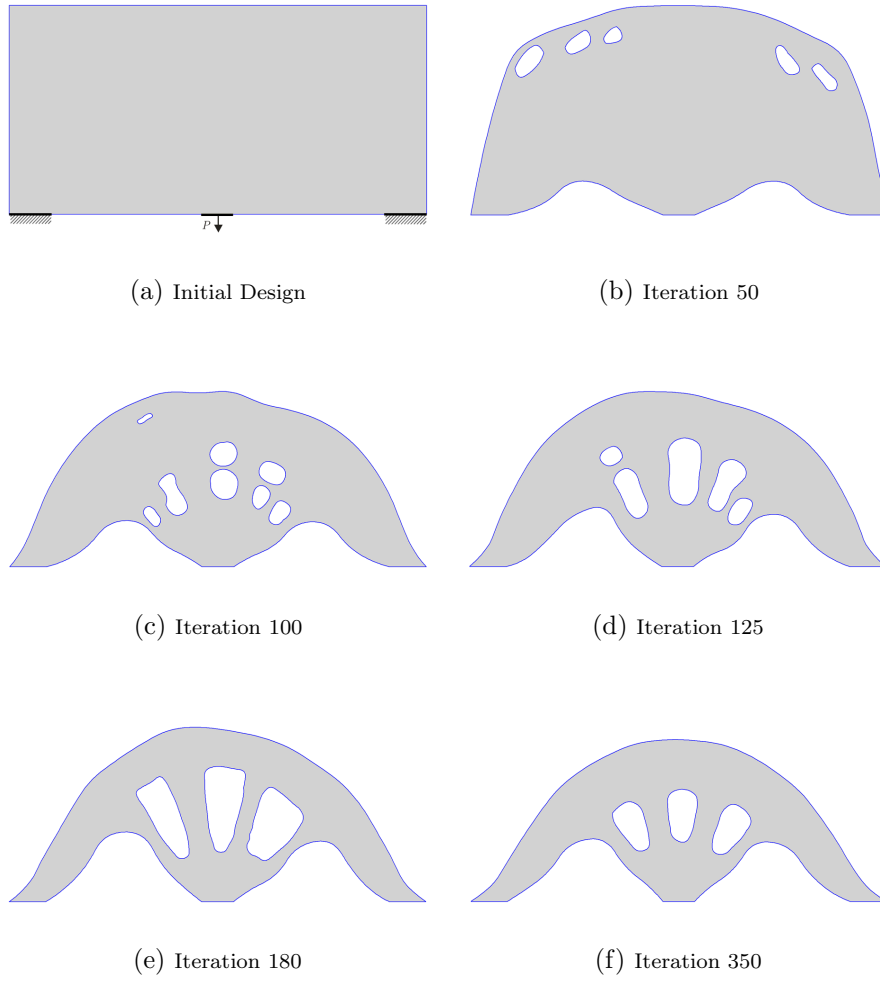


Figure 9: Evolution of structural geometry for Example-4

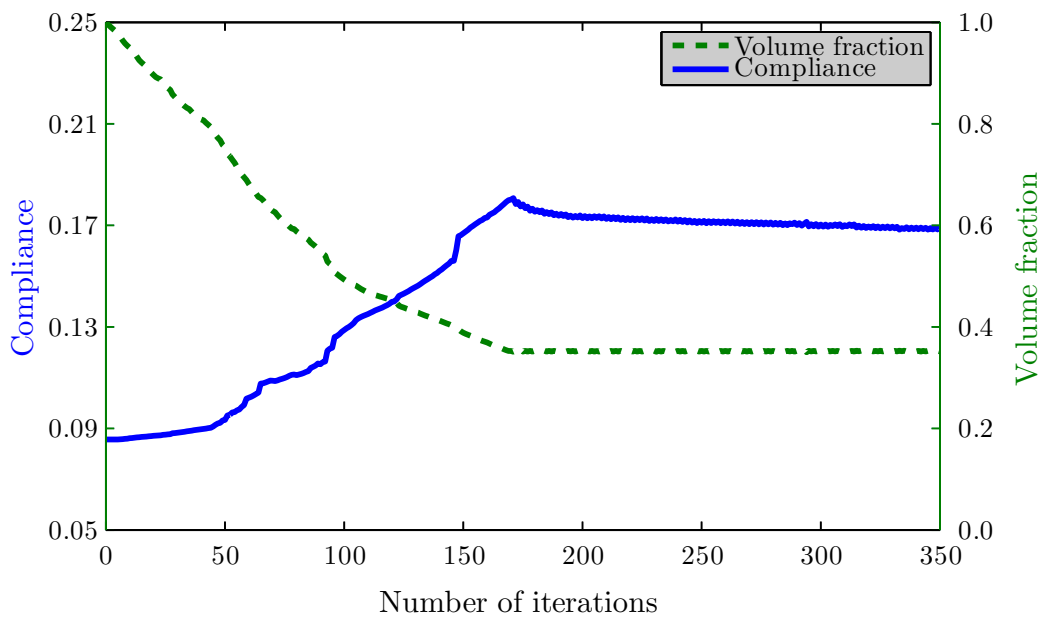


Figure 10: Convergence of objective function and volume for Example-4

## 5. Conclusions

A bi-directional evolutionary structural optimisation method based on the BEM, LSM and NURBS is presented in this paper. The proposed method is capable of nucleating holes during the optimisation process using a stress based hole insertion criterion.

In this paper a volume preserving mechanism is introduced which effectively handles the volume constraint for the solution of minimum compliance problems. The volume preserving mechanism is based on the bisectioning algorithm which precisely adjusts the material removal in accordance with the material addition. Thus, this new implementation fulfills the requirement of a volume preserving technique in a LS and BEM based optimisation method.

The effectiveness of the proposed implementation is demonstrated through the numerical examples presented, which provides smooth convergence of the objective function and better geometrical description of the optimal geometry than that without this implementation. The optimal geometries produced are smoother, and have more uniformly sized members, than those produced without the new adaptation. In addition, this implementation allows us to evaluate the proposed optimisation method for its intended purpose of minimising the the objective function at constant volume, which is of a paramount importance for designing high performance structures.

Numerical examples of two-dimensional structures are chosen to show the computational efficiency (gained through boundary discretisation), convergence speed and insensitivity of the optima to initial designs. Compared with the available BEM and LSM based optimisation methods, the present method generates similar optimal designs rapidly and largely eliminates the depen-

dency on initial guessed designs with pre-existing holes. In addition, the use of NURBS provides optimal designs in a standard CAD format without any intermediate material densities along the structural boundary. Therefore, from an engineering point of view the optimal designs can be easily interpreted and be directly used in other design processes.

### **Acknowledgements**

The first author acknowledges with thanks the financial support through the Durham Doctoral Studentship scheme of the Durham University.

### **References**

- [1] N. P. Dijk, K. Maute, M. Langelaar, F. Keulen, Level-set methods for structural topology optimization: a review, *Structural and Multidisciplinary Optimization* 48 (3) (2013) 437–472.
- [2] M. P. Bendsøe, N. Kikuchi, Generating optimal topologies in structural design using a homogenization method, *Computatr Methods in Applied Mechanics and Engineering* 71 (2) (1988) 197–224.
- [3] O. Sigmund, A 99 line topology optimization code written in Matlab, *Structural and Multidisciplinary Optimization* 21 (2) (2001) 120–127.
- [4] J. A. Sethian, A. Wiegmann, Structural boundary design via level set and immersed interface methods, *Journal of Computational Physics* 163 (2) (2000) 489–528.

- [5] G. Allaire, F. Jouve, A. M. Toader, Structural optimization using sensitivity analysis and a level-set method, *Journal of Computational Physics* 194 (1) (2004) 363–393.
- [6] M. Y. Wang, X. Wang, D. Guo, A level set method for structural topology optimization, *Computer Methods in Applied Mechanics and Engineering* 192 (1-2) (2003) 227–246.
- [7] T. Yamada, K. Izui, S. Nishiwaki, A. Takezawa, A topology optimization method based on the level set method incorporating a fictitious interface energy, *Computer Methods in Applied Mechanics and Engineering* 199 (45-48) (2010) 2876–2891.
- [8] S. Y. Wang, K. M. Lim, B. C. Khoo, M. Y. Wang, An extended level set method for shape and topology optimization, *Journal of Computational Physics* 221 (1) (2007) 395–421.
- [9] S. Osher, J. A. Sethian, Front propagating with curvature-dependent speed: algorithms based on Hamilton-Jacobi formulations, *Journal of Computational Physics* 79 (1) (1988) 12–49.
- [10] K. Abe, S. Kazama, K. Koro, A boundary element approach for topology optimization problem using the level set method, *Communications in Numerical Methods in Engineering* 23 (5) (2007) 405 – 416.
- [11] S. Yamasaki, T. Yamada, T. Matsumoto, An immersed boundary element method for level-set based topology optimization, *International Journal for Numerical Methods in Engineering* 93 (9) (2013) 960–988.

- [12] B. Ullah, J. Trevelyan, I. Ivriissimtzis, A three-dimensional implementation of the boundary element and level set based structural optimisation, *Engineering Analysis with Boundary Elements* 58 (2015) 176–194.
- [13] B. Ullah, J. Trevelyan, A boundary element and level set based topology optimisation using sensitivity analysis, *Engineering Analysis with Boundary Elements* 70 (2016) 80–98.
- [14] K. Abe, T. Fujiu, K. Koro, A be-based shape optimization method enhanced by topological derivative for sound scattering problems, *Engineering Analysis with Boundary Elements* 34 (12) (2010) 1082 – 1091.
- [15] H. Isakari, K. Kuriyama, S. Harada, T. Yamada, T. Takahashi, T. Matsumoto, A topology optimisation for three-dimensional acoustics with the level set method and the fast multipole boundary element method, *Mechanical Engineering Journal* 4 (1) (2014) 1–13.
- [16] G. Jin, H. Isakari, T. Matsumoto, T. Yamada, T. Takahashi, Level set based topology optimisation for 2D heat conduction problem using BEM with objective function defined on design dependent boundary with heat transfer boundary condition, *Engineering Analysis with Boundary Elements* 61 (2016) 61–70.
- [17] S. J. Osher, F. Santosa, Level set methods for optimization problems involving geometry and constraints: I. frequencies of a two-density inhomogeneous drum, *Journal of Computational Physics* 171 (1) (2001) 272 – 288.

- [18] G. Allaire, F. Jouve, A level-set method for vibration and multiple loads structural optimization, *Computer Methods in Applied Mechanics and Engineering* 194 (3033) (2005) 3269 – 3290.
- [19] H. Jia, H. Beom, Y. Wang, S. Lin, B. Liu, Evolutionary level set method for structural topology optimization, *Computers and Structures* 89 (5-6) (2011) 445–454.
- [20] B. Ullah, J. Trevelyan, Correlation between hole insertion criteria in a boundary element and level set based topology optimisation method, *Engineering Analysis with Boundary Elements* 37 (11) (2013) 1457 – 1470.
- [21] Y. M. Xie, G. P. Steven, A simple evolutionary procedure for structural optimization, *Computers and Structures* 49 (1993) 885–96.
- [22] Y. M. Xie, G. P. Steven, Evolutionary structural optimization for dynamic problems, *Computers and Structures* 58 (6) (1996) 1067 – 1073.
- [23] O. M. Querin, G. P. Steven, Y. M. Xie, Evolutionary structural optimisation (ESO) using a bidirectional algorithm, *Engineering Computations* 15 (8) (1998) 1031–1048.
- [24] X. Huang, Y. M. Xie, Convergent and mesh-independent solutions for the bi-directional evolutionary structural optimization method, *Finite Elements in Analysis and Design* 43 (14) (2007) 1039–1049.
- [25] X. Huang, Y. M. Xie, *Evolutionary Topology Optimization of Continuum Structures: Methods and Applications*, New York: John Wiley & Sons, 2010.

- [26] E. Cervera, J. Trevelyan, Evolutionary structural optimisation based on boundary representation of NURBS. Part I: 2D algorithms, *Computers and Structures* 83 (2005) 1902–1916.
- [27] E. Cervera, J. Trevelyan, Evolutionary structural optimisation based on boundary representation of NURBS. Part II: 3D algorithms, *Computers and Structures* 83 (23) (2005) 1917–1929.
- [28] B. Ullah, J. Trevelyan, P. Matthews, Structural optimisation based on the boundary element and level set methods, *Computers & Structures* 137 (2014) 14–30.
- [29] B. Ullah, Structural topology optimisation based on the Boundary Element and Level Set methods, PhD thesis, University of Durham, Durham, UK, 2014.
- [30] J. Trevelyan, "Concept Analyst Ltd". [Online] [www.conceptanalyst.com](http://www.conceptanalyst.com) (2006). [link].  
URL [www.conceptanalyst.com](http://www.conceptanalyst.com)
- [31] Q. Li, G. P. Steven, Y. M. Xie, On equivalence between stress criterion and stiffness criterion in evolutionary structural optimization, *Structural Optimization* 18 (1) (1999) 67–73.
- [32] D. Adalsteinsson, J. A. Sethian, The fast construction of extension velocities in level set methods, *Journal of Computational Physics* 148 (1) (1999) 2–22.
- [33] J. A. Sethian, *Level Set Methods and Fast Marching Methods: Evolving Interfaces in Computational Geometry, Fluid Mechanics, Computer Vi-*

sion, and Materials Science, 2nd Edition, Cambridge University Press, 1999.

- [34] D. F. Rogers, *An Introduction to NURBS: With Historical Perspective*, Morgan Kaufmann, 2001.
- [35] G. Allaire, F. Jouve, Minimum stress optimal design with the level set method, *Engineering Analysis with Boundary Elements* 32 (11) (2008) 909–918.
- [36] L. Carretero Neches, A. P. Cisilino, Topology optimization of 2D elastic structures using boundary elements, *Engineering Analysis with Boundary Elements* 32 (7) (2008) 533–544.